Mon. Not. R. astr. Soc. (1981) **194**, 679–691

The apparent and true ellipticities of galaxies of different Hubble types in the Second Reference Catalogue

James Binney *Princeton University Observatory, Peyton Hall, Princeton, New Jersey 08544, USA*

G. de Vaucouleurs *Department of Astronomy, University of Texas, Austin, Texas 78712, USA*

Received 1980 July 7; in original form 1980 June 10

Summary. We analyse the apparent ellipticities of 1750 galaxies listed in the *Second Reference Catalogue* (RC2) as having diameters in excess of about 2 arcmin to determine the distribution of true ellipticities at nine stages along the Hubble sequence from E to Im. The modal true axial ratio of elliptical galaxies lies near 0.62 irrespective of whether these systems are oblate or prolate. If ellipticals are prolate, the relative frequency of truly spherical galaxies is 50 per cent higher than if they are oblate. The true axial ratios of Magellanic irregulars are approximately uniformly distributed between 0.2 and 0.8. We are unable to obtain statistically satisfactory fits to the data for lenticular galaxies that use only circularly-symmetric bodies with axial ratios smaller than 0.5; we believe this effect is not due to selection against edge-on galaxies but indicates that more than 10 per cent of galaxies classified as S0 are dominated by non-elliptical bulges. Late-type spirals tend to be flatter than the earlier types. The ellipticity distributions favour the possibility that many discs are slightly elliptical.

1 Introduction

The relation between the apparent and the true relative frequency functions of galaxies, particularly ellipticals, has been discussed many times (de Vaucouleurs 1959, 1974, and references therein). The early studies were hampered by the large accidental and systematic errors in the data and the inadequacy of small inhomogeneous samples. The (*First*) *Reference Catalogue of Bright Galaxies* (de Vaucouleurs & de Vaucouleurs 1964) (RC1) provided more homogeneous data for a larger sample than had hitherto been available, and this sample has been analysed by several authors (SFS = Sandage, Freeman & Stokes 1970; vdB = van den Bergh 1977; Noerdlinger 1979). In this paper we explore the still larger and higher quality sample that can be extracted from the *Second Reference Catalogue* (de Vaucouleurs, de Vaucouleurs & Corwin 1976) (RC2) by restricting the analysis to galaxies of large apparent diameter.

The RC2 data are superior to the RC1 data in several respects: (a) The sample is larger; we analyse the data for 1750 galaxies of above-average apparent size, compared with 690 Shapley–Ames objects in the SFS sample and 874 non-selected objects from RC1 in the vdB sample. (b) The ellipticities in the RC2 refer to a statistically well defined isophotal level ($\mu_B = 25.0\,\mathrm{mag\,arcsec^{-2}}$). (c) In the RC2 each axial ratio is associated with a mean error. This enables one to correct for the effects of accidental measuring errors.

This paper differs from an earlier analysis of the RC2 data (de Vaucouleurs & Pence 1973; de Vaucouleurs 1974) in the technique used to derive 'true' ellipticity distributions. De Vaucouleurs & Pence analysed the RC2 data in terms of two-component models of the true ellipticity distributions; in this technique one optimizes the fit to the observations of the projection on to the sky of two-component Gaussian distributions of the true axial ratios. De Vaucouleurs & Pence found that single-component Gaussian distributions do not furnish satisfactory fits to the data for most Hubble type (de Vaucouleurs 1974, 1977). More recently Okamura & Takase (1980) have used similar techniques on a number of small subsets of the RC2 data with similar results. We have sought to clarify the significance of the failure of single-component models adequately to fit the data by employing the non-parametric technique of Lucy (1974) to *invert* the ellipticity distributions of the RC2. Our analysis differs from the work of Noerdlinger (1979), who also used Lucy's inversion algorithm, in that (a) our sample is larger and covers every Hubble type, (b) we make allowance for the effects of accidental and systematic measuring errors, and (c) we discuss the effects of the probable non-axisymmetry of disc galaxies.

2 The inversion procedure

Lucy (1974) has described a general algorithm by which observed distributions may be fit with models of the underlying distributions. Applied to the present problem, Lucy's algorithm involves folding an initial guess at the true ellipticity distribution with the projection probability that a galaxy of known axial ratio is measured to have a certain apparent axial ratio, to obtain a better estimate of the true distribution. One then repeats the procedure starting with the new estimate of the true distribution, to obtain a still better estimate, and so on through as many steps as may be useful. Recently this technique has been employed by Noerdlinger (1979) to invert the ellipticity distributions of SFS and Thompson (1976). The interested reader is referred to the papers of Lucy and Noerdlinger for details. We confine discussion here to two respects in which our procedure differs from that of Noerdlinger.

2.1 ALLOWANCE FOR MEASURING ERRORS

It is likely that there is a systematic tendency for the ellipticities of nearly circularly-symmetric galaxies to be overestimated. This will undoubtedly be the case if the principal axes are sought by the repeated measurement of different diameters until the two orthogonal diameters are found that have the greatest value of R ($=D/d = a/b = q^{-1}$). And even if such a search is not explicit, it is probable that the eye locates candidate principal axes by a similar process. In our analysis of the data we have attempted to correct for this effect by reducing all values of $\log R$ in the range $0.01 < \log R < 0.04$ by 0.005. (Note that $\log R$ is given to nearest 0.01 only in RC2.)

When $\log R > 0.04$ the orientation of the principal axes should be fairly unambiguous, with the result that we may suppose the errors to be approximately randomly distributed in $\log R$ with a mean error of 0.03 in our samples. If we assume a simple form for the

probability $E(q|q')\,\delta q$ that a galaxy of apparent axial ratio q' is actually measured to have axial ratio q, then we may structure Lucy's algorithm so that it makes full allowance for accidental measuring errors.

We adopt for the probability density $E(q|q')$

$$E(q|q') = (\sqrt{2\pi}\,\sigma)^{-1}\ (\exp[-(q-q')^2/2\sigma^2] + \exp[-(2-(q+q')^2)/2\sigma^2]), \tag{1a}$$

where

$$\sigma(q') = 0.07\,q' \tag{1b}$$

which approximately corresponds to a dispersion of 0.03 in $\log R$. The second term on the right hand side of equation (1a) represents the probability that measuring errors have reversed the roles of the apparent major and minor axes of a nearly round galaxy. With this choice of E one has for the probability $P(q|\xi)\,\delta q$ that a galaxy known to have true axial ratio ξ is measured to have apparent axial ratio near q

$$P(q|\xi) = \int_{\xi}^{1} E(q|q')\,p(q'|\xi)\,dq'. \tag{2}$$

Here $p(q'|\xi)\,\delta q'$ is the probability that a galaxy of true axial ratio ξ is projected such that it has apparent axial ratio near q'. By employing in Lucy's equations $P(q|\xi)$ as given by equations (1) and (2) in place of the error-free projection kernels $p(q'|\xi)$ we make full allowance for accidental measuring errors.

In common with other workers we assume a random orientation of the principal axes of the galaxies to the line of sight. This assumption has been questioned by Reinhardt & Roberts (1972) and by de Vaucouleurs (1978), but the suspected departures, if real, are not large. We further assume that the isophotal surfaces of galaxies of all types can be approximated by ellipsoids. Okamura & Takase (1980) find that simple ellipsoidal models generally fit the data at least as well as more sophisticated disc-plus-bulge models. With these assumptions the kernels $p(q'|\xi)$ are those given by Hubble (1926), Heidmann, Heidmann & de Vaucouleurs (1971) or Binney (1978b), depending on whether the galaxies are to be modelled with oblate or prolate figures of revolution. Notice that the error-corrected projection kernel $P(q|\xi) \neq 0$ for $q < \xi$, and that this necessitates extension of the range of integration employed by Noerdlinger (1979).

2.2 CONSIDERATION OF TRIAXIAL SYSTEMS

The possibility that elliptical galaxies are triaxial has recently been widely discussed (for a review see Binney 1979). Unfortunately ellipticity distributions alone can throw little light on this interesting question (Binggeli 1980). But it is valuable to pursue the possibility raised in an earlier paper (Binney 1978a) that disc galaxies may not be circularly-symmetric. With this aim in view we have calculated the probability $p_t(q'|\xi,\zeta)\,\delta q'$ that a triaxial galaxy whose principal axes have lengths in the ratio $1:\zeta:\xi$ $(1>\zeta>\xi)$ is projected to apparent axial ratio q':

$$p(q\,|\,\xi,\zeta) = \frac{2}{\pi}\int_{\theta_1}^{\theta_2} \frac{\partial(\phi,\theta)}{\partial(q,\theta)}\sin\theta\,d\theta, \tag{3}$$

$$= \frac{2}{\pi}\int_{\theta_1}^{\theta_2} \left(\frac{\partial q}{\partial\phi}\right)_{\theta}^{-1}\sin\theta\,d\theta.$$

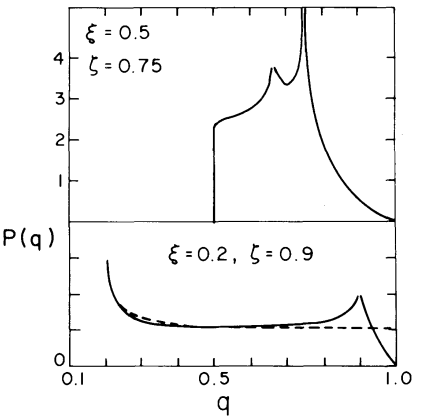

Figure 1. The probability density that a triaxial ellipsoid whose body axes have lengths in the ratio $\xi:\xi:1$ has apparent axial ratio q. The dashed curve in the lower panel is the probability density for an oblate spheroid of true axial ratio $\xi = 0.2$.

In equation (3) $q(\theta, \phi; \xi, \zeta)$ is the apparent axial ratio of a triaxial ellipsoidal galaxy which is oriented such that θ and ϕ are the polar coordinates of the line of sight with respect to the body axes (the z- and x-axes are respectively the shortest and longest body axes). The integral is over the range of values of θ ($\theta_1 \leqslant \theta \leqslant \theta_2$) for which there exists an angle ϕ at which the body appears to have the stated axial ratio. Details of the integrand in equation (3) and of the angles θ_1 and θ_2 will be found in the Appendix.

In Fig. 1 we show two examples of the projection probability densities of triaxial configurations. Notice that these differ from the probability densities of biaxial systems in two respects: (1) The projection probability of a triaxial body peaks at two apparent axial ratios; these peaks coincide with the two greatest of the apparent axial ratios of the body when it is viewed along its body axes ($\zeta, \xi/\zeta, \xi$). The smallest principal axial ratio is not particularly favoured. (2) The probability of observing a triaxial body to be nearly round is very small. Thus if apparently round elliptical galaxies seem to be intrinsically different from apparently elongated galaxies (Terlevich *et al.* 1980) this might be taken as evidence that some elongated galaxies are actually triaxial.

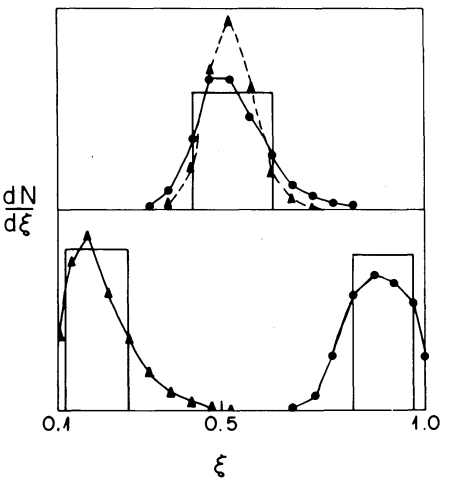

Figure 2. Tests of the inversion algorithm. The points in the upper panel are the inversions of two sets of pseudo-data generated by randomly projecting oblate spheroids whose true axial ratios ξ are drawn from the rectangular distribution shown. The lower panel shows inversions of two similar pseudo-data sets (*cf.* Table 1).

Table 1. Parameters of fits to pseudo-data.

Data set	True range ξ_1	ξ_2	χ^2/bin	P_{ks}
1	0.43	0.62	0.46	0.41
2	0.43	0.62	1.0	0.16
3	0.12	0.27	0.46	0.10
4	0.82	0.98	0.62	0.31

We have tested the effectiveness of the deprojection algorithm by attempting to recover the probability distributions underlying sets of pseudo-data. Fig. 2 shows the results of four such tests. The rectangles show the probability distributions of true axial ratios according to which sets of 200 galaxies were assigned apparent axial ratios that incorporated similar accidental measuring errors to those in the RC2 data. The points in the upper panel show the inversion of two such data sets for one underlying distribution. Typically 10–20 cycles of the inversion algorithm were required to produce the results shown in Fig. 2.

We have used two criteria for judging the quality of derived distributions: (i) The standard χ^2 statistic, and (ii) a modified Kolmogorov–Smirnov statistic, in which we treat the distribution predicted by projecting the derived true distribution back on to the plane of the sky, as an observed distribution, and then calculate the probability (denoted P_{ks} below) that two independent realizations of the same (unknown) probability distribution would differ by at least as much as the observed and predicted distributions. At first sight this Kolmogorov–Smirnov statistic would not appear to be a very rigorous test of the derived distribution. However, one finds in practice that it is in many cases harder to satisfy the criterion that there be an appreciable Kolmogorov–Smirnov probability than to achieve a satisfactory χ^2 value. Indeed we shall see below that there is a tendency for some predicted distributions to be systematically deficient in apparently nearly round galaxies. Within any one bin the deficiency may not be statistically significant, although a similar deficiency in several adjacent bins may be significant. The Kolmogorov–Smirnov test is well adapted to detecting such systematic trends. Table 1 gives values of χ^2 per bin and P_{ks} for the fits shown in Fig. 2. These may be taken as indicative of the quality of fit that can be achieved by Lucy's algorithm when the data are consistent with the probability distribution used in the inversion.

3 Application to the RC2 data

Table 2 lists the numbers of galaxies in RC2 that have corrected diameters D_0 larger than the median $\dot{D}_0$ at each Hubble stage, and their distribution with respect to apparent axial ratio R. Some Hubble stages have been grouped to improve the statistics and we have excluded the Local Group dwarf spheroidal galaxies. Histograms of the data after correction as described in Section 2.1 for systematic errors near $q = 1$ are shown in the upper panels of Figs 3–7.

We have made no corrections for possible selection effects because (i) our sample is largely selected by corrected face-on diameter, and (ii) the restriction to apparently large galaxies automatically eliminates most of the biases that could affect smaller, fainter objects. Indeed the mean apparent ellipticity of each type is constant and independent of D_0 down to diameters somewhat smaller than the median $\dot{D}_0$. Therefore it seems safe to assume that selection is by corrected apparent diameter alone, in which case no correction for differential selection by ellipticity is required.

Table 2. Frequencies of axial ratios $R = a/b$ from the *Second Reference Catalogue*.★

t	−6, −5, −4	−3, −2, −1	0, 1	2	3	4	5	6, 7	8, 9, 10
$\dot{D}_0$ (arcmin)	2.1	1.9	1.9	2.0	2.0	2.3	2.3	2.4	1.9
$\log R < 0.025$	33	19	8	5	9	7	9	6	28
0.025–0.045	28	20	4	6	9	8	20	10	10
0.045–0.075	19	29	23	5	19	21	14	15	27
0.075–0.095	18	20	13	5	6	6	11	7	16
0.095–0.125	25	31	17	8	16	9	17	10	21
0.125–0.155	16	20	10	10	12	12	10	13	23
0.155–0.185	16	20	12	1	19	12	17	8	11
0.185–0.225	23	19	11	5	19	9	13	13	20
0.225–0.265	9	19	14	9	19	10	19	9	13
0.265–0.305	5	13	17	4	12	10	11	11	8
0.305–0.345	1	15	8	5	10	7	12	4	9
0.345–0.395	3	13	17	8	8	11	10	5	9
0.395–0.455	0	25	14	9	14	15	9	7	5
0.455–0.525	0	18	14	7	9	10	10	9	7
0.525–0.605	0	13	6	4	16	5	9	8	5
0.605–0.695	0	8	1	6	17	3	9	8	3
0.695–0.825	0	1	0	0	10	1	8	9	2
$\log R > 0.825$	0	0	0	0	2	0	1	3	0
N (total)	196	303	189	97	226	156	209	155	217

★ Galaxies having corrected diameters $D_0 > \dot{D}_0$ only.

3.1 ELLIPTICAL GALAXIES

Fig. 3 shows distributions of oblate and prolate spheroids that provide good fits to the data for elliptical galaxies. The points are crude density-values recovered by Lucy's algorithm and the smooth curves represent hand fits to these points that are equally acceptable from the statistical point of view (Table 3). The distributions are qualitatively very similar to those estimated by other authors (Sandage *et al.* 1970; de Vaucouleurs 1974; Binney 1978a). We confirm that the modal ellipticity is 0.38 (E3.8) for both oblate and prolate spheroids, but in all cases there is a significant number of spherical objects.

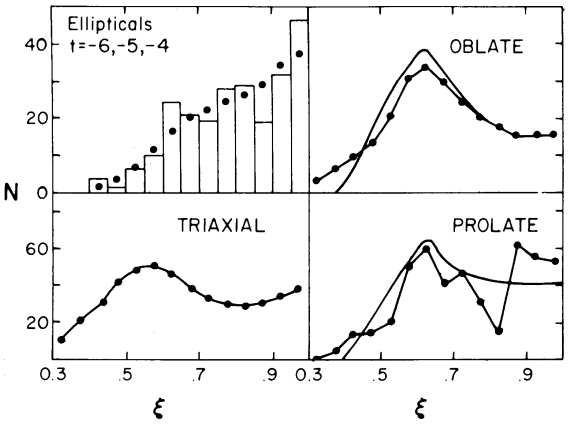

Figure 3. Inversions of the data for elliptical galaxies. The points are automatically recovered inversions. The smooth curves represent statistically acceptable hand fits to these distributions. The points in the upper left hand panel show the fit afforded by the hand fit to the oblate inversion. The lower left hand panel shows the distribution of shortest axial ratios ξ required to fit the data with triaxial ellipsoids whose middle axes have length ζ equal to the average lengths of the greatest and shortest axes (*cf.* Table 3).

The lower left hand panel in Fig. 3 shows a distribution of triaxial ellipsoids, each of which has $\zeta = \frac{1}{2}(1 + \xi)$, that fits the data well. Benacchio & Galletta (1980) have used these same ellipsoids to fit the data of Strom & Strom (1978a, b, c) with very different results; their true distribution contains very few nearly spherical galaxies. This appears to be because their observed distribution, unlike ours, is very poor in round systems.

3.2 LENTICULAR GALAXIES

The dots joined by full lines in Fig. 4 show the ellipticity distribution recovered by Lucy's algorithm under the assumption that lenticular galaxies may be represented by oblate spheroids without any restriction as to the permitted true axial ratio values. There appear to be two components to the distribution of true axial ratios; a narrow component centred on $\xi = 0.27$ and that is 0.1 in half-width, and a broad component that reaches out to $\xi = 0.8$.

Table 3. Fits to data for elliptical galaxies.

Type	Free fit		Hand fit	
	χ^2/bin	P_{ks}	χ^2/bin	P_{ks}
Oblate	0.84	0.72	0.80	0.62
Prolate	0.92	0.22	0.76	0.72
Triax	0.88	0.72	–	–

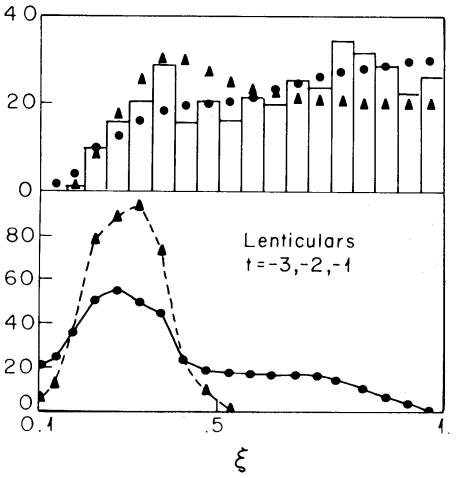

Figure 4. Fits to the data for lenticular galaxies. The dots joined by full lines in the upper and lower panels represent a free fit of spheroids. The triangles joined by broken lines in these panels represent the best fit obtainable using only spheroids flatter than $\xi = 0.5$ (*cf.* Table 4).

This distribution is in good agreement with the findings of de Vaucouleurs & Pence (1973), and of Okamura & Takase (1980), but not with that of Noerdlinger (1979). There can be no doubt that the data histogrammed in Fig. 4 do require the existence of lenticular galaxies rounder than $\xi = 0.5$; the triangles in that figure show the best fit that can be obtained when one restricts oneself to spheroids flatter than $\xi = 0.5$. This fit is rated poor by the χ^2 test and entirely ruled out by the Kolmogorov–Smirnov test (Table 4) because, as Fig. 4 indicates, this model furnishes too many apparently elongated systems and too few nearly round ones.

Therefore it seems likely that our sample really does contain some rather spherical systems whose light distributions interior to the $\mu_B = 25$ isophote are entirely dominated by their bulge components. This being so, the S0 classifications of these systems must rest on features in their brightness profiles that are intrinsic to the bulge components; thus these features are to be distinguished from the more familiar features that arise for flattened lenticular or spiral galaxies at the radius where the overall profile switches from being dominated by the bulge at small radii to being dominated by an exponential disc further out. In fact, the foregoing suggests that these rather spherical S0 galaxies may not possess disc components at all. Possible examples of 'discless' lenticulars include NGC 404, 2855, 3032, 4459, 5273 (illustrated in the *Hubble Atlas*).

Table 4. Fits to data for lenticular, spiral and irregular galaxies.

Class	Spheroidal Free fit		Spheroidal Restricted fit		Triaxial Restricted fit		
t	χ^2/bin	P_{ks}	χ^2/bin	P_{ks}	ξ	χ^2/bin	P_{ks}
−1, −2, −3	0.8	0.35	1.5	0	–	–	–
0, 1	0.99	0.14	1.2	0.38	0.9	0.84	0.30
2	0.91	0.27	0.78	0.41	–	–	–
3	0.85	0.21	1.0	0.07	0.9	0.96	0.48
4	0.73	0.51	0.8	0.12	–	–	–
5	0.60	0.43	0.86	0.01	0.9	1.0	0.17
6, 7	0.54	0.51	0.77	0.004	0.9	0.75	0.08
8, 9, 10	0.96	0.35	–	–	–	–	–

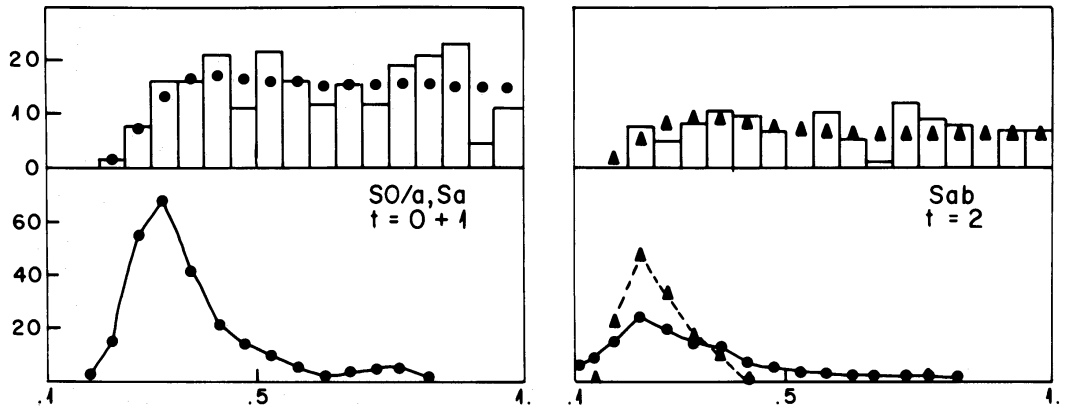

Figure 5. Fits to the data for early-type spirals. The dots joined by full lines represent free fits of spheroids. The triangles joined by dashed lines represent a fit that uses only spheroids flatter than $\xi = 0.5$.

3.3 SPIRAL GALAXIES

In Figs 5 and 6 we show the data and a number of inversions for galaxies of Hubble types between $t = 0$ and $t = 7$. The inversions obtained for each of these six data sets (filled circles joined by full lines) by fitting with spheroids of unconstrained axial ratios, show tails of only slightly flattened systems similar to, though less pronounced than, that discussed above for the lenticulars. There is a tendency for the axial ratio ξ_{max} at which the distributions peak

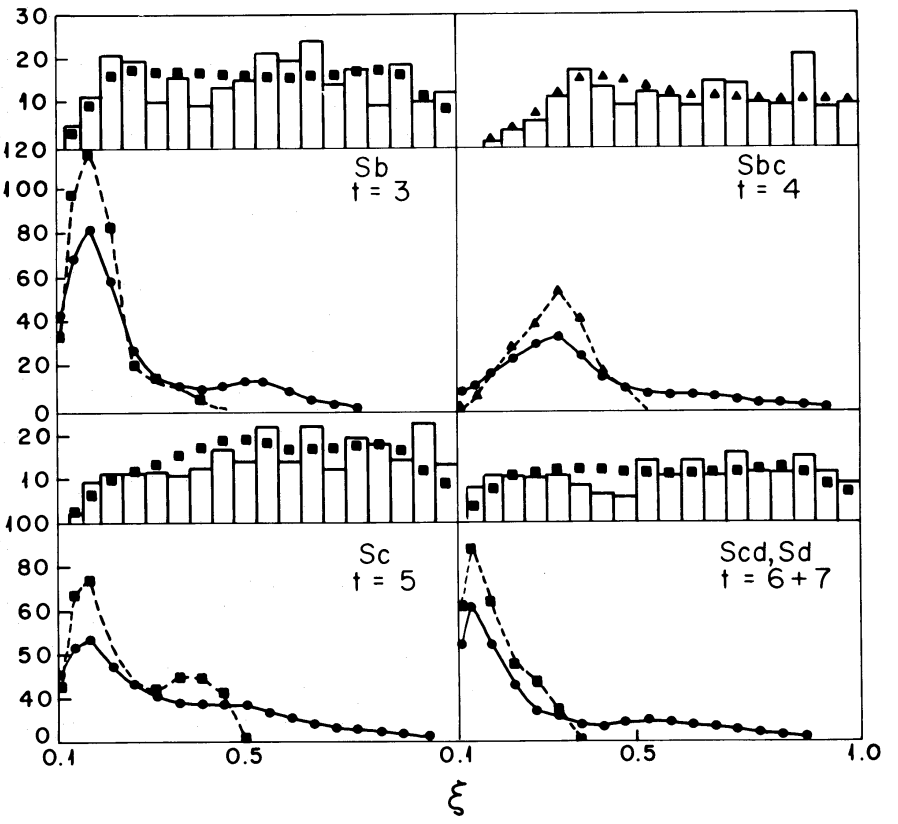

Figure 6. Fits to the data for intermediate- and late-type spirals. The dots joined by full lines represent free fits of spheroids. The triangles show the best fits obtained using only spheroids flatter than $\xi = 0.5$, and the squares show fits using triaxial bodies (*cf.* Table 4).

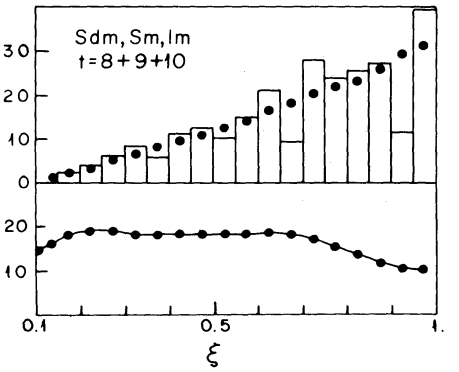

Figure 7. Fit to the data for very late-type galaxies using only oblate spheroids.

to decrease from $\xi_{max} = 0.35$ for the $t = 0 + 1$ class to $\xi_{max} = 0.15$ for the $t = 6 + 7$ class. However, the $t = 4$ class with $\xi_{max} = 0.2$ does not accord with this trend.

Intuitively one would hope to be able to model all spirals later than Sb ($t = 3$) employing only spheroids flatter than $\xi = 0.5$. The triangles in the panels of Figs 5 and 6 that relate to the classes $t = 0 + 1$, $t = 2$ and $t = 4$ show fits of this type that are satisfactory from the points of view of both the Kolmogorov–Smirnov and the χ^2 tests. These distributions closely resemble the unrestricted fits after removal of their tails.

Table 4 shows that for the classes $t = 3$, $t = 5$ and $t = 6 + 7$ no adequate fit is obtainable that uses only flat axisymmetric spheroids; the χ^2 can be satisfactory, but the fits fail the Kolmogorov–Smirnov test (*cf.* Table 1). Fig. 6, particularly the panel for the classes $t = 3$ and $t = 6 + 7$ suggest that the problem may be a dearth of apparently round systems. This observation and Fig. 1 suggest that one try fitting the data for these classes with elliptical discs. From a physical point of view non-axisymmetry might be due to either (1) superficial spiral structure or (2) rotation of the entire disc in the non-axisymmetric gravitational field of a bar or a triaxial heavy halo (Binney 1978a). Table 4 and the squares in Fig. 6 show that models of this type do fit the data better than do axisymmetric spheroids. Indeed the classes $t = 0 + 1$, $t = 3$ and $t = 5$ are well fit by distributions of flat ($\xi < 0.5$) elliptical ($\zeta = 0.9$) ellipsoids. The fit to the class $t = 6 + 7$ with elliptical discs is less good ($P_{ks} = 0.08$) but nevertheless better than the fit with axisymmetric spheroids ($P_{ks} = 0.004$). Figs 1 and 4 indicate that some lenticular galaxies may be triaxial, with $\zeta = 0.8$ because the apparent frequency distribution for this class declines beyond $q = 0.8$, but one cannot obtain a satisfactory fit to the lenticulars using only flattened elliptical systems; there are simply too many galaxies seen at $q > 0.5$. Likewise, Figs 5 and 6 indicate that few spirals can exist whose discs are more elliptical than $\zeta = 0.9$.

3.4 MAGELLANIC IRREGULARS

Fig. 7 shows the apparent and true distributions for 217 galaxies of types $t = 8$, 9 and 10. The steady increase in the number density of galaxies from $q = 0.1$ to $q = 0.75$ necessarily leads to a rather uniform distribution of true ellipticities. Thus many very late-type galaxies are not disc galaxies. The spiral structure observed in galaxies of types Sdm and Sm ($t = 8$, 9) (de Vaucouleurs & Freeman 1972) suggests that galaxies of these types do possess discs, and therefore implies that the more spherical galaxies are concentrated into type Im ($t = 10$).

This morphological conclusion is confirmed by the available dynamical evidence: If the random velocities of interstellar clouds are set by gas dynamic processes, such as acceleration by supernova shock waves (e.g. Jenkins, Silk & Wallerstein 1977), that are independent of the depth of the galactic potential well, then the clouds in irregular systems will have similar random velocities ($\Delta v \approx 10$–$15\,\mathrm{km\,s^{-1}}$) to those of clouds in our own galaxy. But the

rotation velocities characteristic of many irregular systems are only $v \approx 20\,\mathrm{km\,s^{-1}}$ (Tully *et al.* 1978). Therefore the Population I material of many very late type galaxies is probably characterized by too large a ratio of random to rotational kinetic energy to form a more than moderately flattened subsystem.

Hence it seems that many Magellanic irregulars resemble elliptical galaxies in shape. However, in another important respect they are unlike elliptical galaxies; their rotation curves are almost linear out to the Holmberg radius (Tully *et al.* 1978). This phenomenon may arise because the large random motions and appreciable collision cross-sections of the clouds in these systems give rise to a high effective viscosity; angular momentum will be redistributed through the system until solid body rotation is established and the mean velocity field becomes shear free. The tendency of late-type galaxies to have bars (de Vaucouleurs & Freeman 1972) is possibly a consequence of their near solid-body rotation (*cf.* Kormendy & Norman 1979).

5 Conclusions

We have analysed the ellipticity distributions of 1750 galaxies from the *Second Reference Catalogue*. This sample, which contains only galaxies whose corrected face-on diameters D_0 exceed about 2 arcmin, is substantially free from bias. We assume that the symmetry axes are randomly oriented to infer true axis-ratio distributions at nine stages along the Hubble sequence.

The results obtained are simplest at the two extremes of the Hubble sequence. The apparent ellipticities of elliptical galaxies may be satisfactorily accounted for in terms of a distribution of either oblate or prolate spheroids that peaks near true axis ratio $\xi = 0.62$ (E3.8) and falls to zero by $\xi = 0.35$ (E6.5) in the oblate case, or $\xi = 0.4$ (E6) in the prolate case. Both distributions involve some spherical galaxies, although these are not very common in the oblate case. Alternatively triaxial ellipsoids may account for the data. If elongated ellipticals are generally strongly triaxial, most apparently round galaxies must be truly spherical.

There is clear evidence that there are many thick galaxies at the very late end of the Hubble sequence. Galaxies of types 8, 9 and 10 occur with about equal frequency at all true axial ratios in the interval $0.1 < \xi < 0.8$. It seems likely that this thickening at late Hubble types is a direct consequence of the low rotation speed and disordered velocity fields observed in Magellanic irregulars.

The situation as regards the lenticular galaxies is more complex. Direct inversion of the observed ellipticity distribution leads to a distribution that is peaked around true axial ratio $\xi = 0.32$, but involves a long tail of more nearly spherical galaxies running out to $\xi = 0.8$. We believe that this tail at large values of ξ is not due to our sample selecting against highly inclined galaxies. Therefore it seems likely that some galaxies classified as lenticulars are nearly spherical. We give a number of possible examples.

Free fits to the apparent ellipticity distributions of spiral galaxies yield distributions of true axial ratios ξ which peak in the range $0.15 \leqslant \xi \leqslant 0.35$. There is a tendency for the later-type spirals to have distributions that peak at smaller (flatter) ξ. Attempts to fit the apparent distributions of several Hubble types using only spheroids flatter than $\xi < 0.5$ produce marginal or even unacceptable fits. Better fits can in each case be obtained with slightly elliptical discs. Large disc ellipticities are, however, incompatible with the data.

Acknowledgment

This work was supported at Princeton under NSF grant AST 79-22074.

References

Benacchio, L. & Galletta, G., 1980. *Mon. Not. R. astr. Soc.*, **193**, 885.
Binggeli, B., 1980. *Astr. Astrophys.*, **82**, 289.
Binney, J. J., 1978a. *Mon. Not. R. astr. Soc.*, **183**, 501.
Binney, J. J., 1978b. *Mon. Not. R. astr. Soc.*, **183**, 779.
Binney, J. J., 1979. *Comments Astrophys.*, **8**, 27.
de Vaucouleurs, G., 1959. In *Handbuch der Physik*, vol. LIII, p. 303, Springer, Berlin.
de Vaucouleurs, G., 1974. In *The Formation and Dynamics of Galaxies*, p. 1, ed. Shakeshaft, J. R., Reidel, Dordrecht.
de Vaucouleurs, G., 1977. In *The Evolution of Galaxies and Stellar Populations*, p. 74, eds Tinsley, B. M. & Larson, R. B., Yale Univ. Obs., New Haven.
de Vaucouleurs, G., 1978. In *The Large Scale Structure of the Universe*, p. 206, eds Longair, M. S. & Einasto, J., Reidel, Dordrecht.
de Vaucouleurs, G. & de Vaucouleurs, A., 1964. *Reference Catalogue of Bright Galaxies*, University of Texas Press, Austin.
de Vaucouleurs, G., de Vaucouleurs, A. & Corwin, H. G., 1976. *Second Reference Catalogue of Bright Galaxies*, University of Texas Press, Austin.
de Vaucouleurs, G. & Freeman, K. C., 1972. Structure and dynamics of barred spiral galaxies, in particular of the Magellanic type, in *Vistas Astr.*, **14**, 163, ed. Beer, A., Pergamon Press, Oxford.
de Vaucouleurs, G. & Pence, W. D., 1973. *Bull. Am. astr. Soc.*, **5**, Part I, 446.
Heidmann, J., Heidmann, N. & de Vaucouleurs, G., 1971. *Mem. R. astr. Soc.*, **76**, 121.
Hubble, E. P., 1926. *Astrophys. J.*, **64**, 321.
Jenkins, E. B., Silk, J. & Wallerstein, G., 1976. *Astrophys. J. Suppl.*, **32**, 618.
Kormendy, J. & Norman, C. A., 1979. *Astrophys. J.*, **233**, 539.
Lucy, L. B., 1974. *Astr. J.*, **79**, 745.
Noerdlinger, AP. D. 1979. *Astrophys. J.*, **234**, 802.
Okamura, S. & Takase, B., 1980. *Publs astr. Soc. Japan*, in press.
Reinhardt, M. & Roberts, M. S., 1972. *Astrophys. Lett.*, **12**, 201.
Sandage, A., Freeman, K. C. & Stokes, N. R., 1970. *Astrophys. J.*, **160**, 831.
Stark, A. A., 1977. *Astrophys. J.*, **213**, 368.
Strom, K. M. & Strom, S. E., 1978a. *Astrophys. J.*, **83**, 73.
Strom. K. M. & Strom, S. E., 1978b. *Astrophys. J.*, **83**, 732.
Strom, K. M. & Strom, S. E., 1978c. *Astrophys. J.*, **83**, 1239.
Terlevich, R., Davies, R., Burstein, D. & Faber, S., 1980. Preprint.
Thompson, L. A., 1976. *Astrophys. J.*, **209**, 22.
Tully, R. B., Bottinelli, L., Fisher, J. R., Gouguenheim, L., Sancisi, R. & van Woerden, H., 1978. *Astr. Astrophys.*, **63**, 37.
van den Bergh, S., 1977. *Observatory*, **97**, 81.

Appendix: Projection probability of triaxial ellipsoid

Let the principal axes of the ellipsoid be in the ratio $1:\zeta:\xi$. Then when one views the body along the longest axis (x-axis) it has apparent axial ratio $\beta_x = \xi/\zeta$. Define similarly $\beta_y = \xi$ and $\beta_z = \zeta$. The formulae given by Stark (1977) show that the integrand of equation (3) is given by

$$\left(\frac{\partial q}{\partial \phi}\right)^{-1} = (A+B)\,(A^2 - B^2)^{1/2} \Big/ \left(B\frac{\partial A}{\partial \phi} - A\frac{\partial B}{\partial \phi}\right), \tag{A1a}$$

where

$$A \equiv \xi^2 \sin^2\theta + \cos^2\phi(\zeta^2 + \cos^2\theta) + \sin^2\phi(1 + \zeta^2\cos^2\theta) \tag{A1b}$$

and

$$B^2 \equiv [\xi^2 \sin^2\theta + \sin^2\phi(\zeta^2\cos^2\theta - 1) + \cos^2\phi(\cos^2\theta - \zeta^2)]^2 + (1-\zeta^2)^2 \sin^2 2\phi \cos^2\theta. \tag{A1c}$$

Consider first the case $\beta_z > \beta_x > \beta_y$. Then to find the limits of the integration in equation (3) of the text one must distinguish three cases:

(a) $q > \beta_z$. In this case the line of sight must be confined to one of four approximately circular annuli around the directions where the body appears to be round. These directions lie in the (x, z) plane (see, e.g. Fig. 2 of Binggeli 1980). Consideration of the geometry of the (x, z) plane shows that the annuli in question intersect the (x, z) plane at

$$\theta_1 = \arcsin\left(\frac{1-\zeta^2/q^2}{1-\xi^2}\right)^{1/2} \tag{A2a}$$

and

$$\theta_2 = \arcsin\left(\frac{1-\zeta^2 q^2}{1-\xi^2}\right)^{1/2}. \tag{A2b}$$

(b) $\beta_z > q > \beta_x$. In this case the line of sight is confined to a band that runs around the z-axis of the ellipsoid. This band crosses the (x, z) plane at a point that lies below the direction at which the body appears to be round, and then rises to cross the (y, z) plane at a smaller value of θ. Thus θ_2 is still given by equation (A2b), whilst consideration of the geometry of the (y, z) plane shows that in this case θ_1 is given by

$$\theta_1 = \arcsin\left(\frac{\zeta^2-q^2}{\zeta^2-\xi^2}\right)^{1/2}. \tag{A3}$$

(c) $\beta_x > q > \beta_y$. The line of sight is now confined to an annulus around the y-axis. This band achieves its greatest and least θ-values where it crosses the (y, z) plane. Thus θ_1 is given by equation (A3) and $\theta_2 = \pi/2$.

When $\beta_x > \beta_z > \beta_y$ we have: (a) If $q > \beta_x$, θ_1 and θ_2 are determined as in case (a) above. (b) If $\beta_x > q > \beta_z$, θ_1 is given by equation (A2a) and $\theta_2 = \pi/2$. (c) If $\beta_z > q > \beta_y$, θ_1 and θ_2 are determined as in case (c) above.